Proton Plasma Asymmetries between the Convective-Electric-Field Hemispheres of Venus' Dayside Magnetosheath

Sebastián Rojas Mata[1,2], Gabriella Stenberg Wieser[1], Tielong Zhang[3], and Yoshifumi Futaana[1]

[1]Swedish Institute of Space Physics, Kiruna, Sweden
[2]Now at KTH Royal Institute of Technology, Stockholm, Sweden
[3]Space Research Institute, Austrian Academy of Science, Graz, Austria

Correspondence: Sebastián Rojas Mata (serm@kth.se)

Abstract. Proton plasma asymmetries with respect to the convective electric field ($\mathbf{E}$) are characterized in Venus' dayside magnetosheath using measurements taken by an ion mass-energy spectrometer and a magnetometer. Investigating the spatial structure of the magnetosheath plasma in this manner provides insight into the coupling between solar-wind protons and planetary ions. A previously developed methodology for statistically quantifying asymmetries is further developed and applied to an existing database of proton bulk-parameter measurements in the dayside magnetosheath. The density and speed exhibit ~~weak~~ mild asymmetries favoring the hemisphere in which $\mathbf{E}$ points towards the planet, while the ~~magnetic-field strength has a weak asymmetry favoring~~ magnetic-field-strength asymmetry favors the opposite hemisphere. The ~~temperatures perpendicular and~~ temperature perpendicular to the background magnetic field has a mild asymmetry favoring the hemisphere in which $\mathbf{E}$ points away from the planet; the temperature parallel to the background magnetic field ~~as well as their ratio~~ and the temperature anisotropy present no significant asymmetries. Deflection of the solar wind due to momentum exchange with planetary ions is revealed by ~~(1)~~ the O^+ Larmor-radius trends of the asymmetries of the bulk-velocity components perpendicular to the upstream solar-wind flow~~and (2) the $\mathbf{E} \times \mathbf{B}_{IMF}$-drift trends of the bulk-velocity component along the cross-flow component of the interplanetary magnetic field ($\mathbf{B}_{IMF}$). These interpretations are~~ . This interpretation is enabled by comparisons to experimental and numerical studies of solar-wind deflection at Mars~~and comet 67P/Churyumov-Gerasimenko~~, highlighting the benefits of comparative planetology studies.

1 Introduction

Unmagnetized bodies like Venus and Mars experience a closer interaction with the solar wind than those with an intrinsic magnetic field (Russell et al., 2016; Futaana et al., 2017). The upstream interplanetary magnetic field (IMF) $\mathbf{B}_{IMF}$ and convective electric field $\mathbf{E} = -\mathbf{v}_{SW} \times \mathbf{B}_{IMF}$ (where $\mathbf{v}_{SW}$ is the solar-wind velocity, see Fig. 1) influence several phenomena such as plasma boundary morphology (Phillips et al., 1986; Zhang et al., 1991b; Edberg et al., 2009; Chai et al., 2015; Signoles et al., 2023), pick-up ion dynamics (Barabash et al., 2007b, a; Brain et al., 2016; Jarvinen et al., 2016), and plasma wave activity (Du et al., 2010; Delva et al., 2011; Ruhunusiri et al., 2017; Xiao et al., 2018). In particular, the structure of the magnetosheath, the region where the solar wind transfers momentum and energy to the planet's magnetosphere (Longmore et al., 2005; Lucek et al., 2005; Haaland et al., 2017), is responsive to the configuration of the upstream electromagnetic fields. For example,

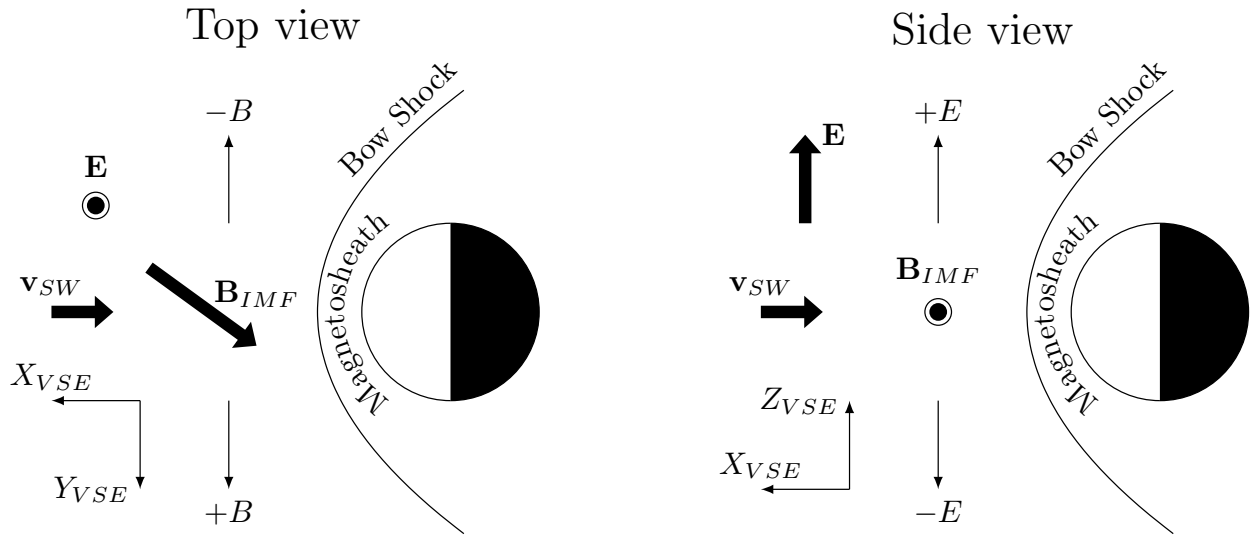

Figure 1. Configuration of electromagnetic fields around Venus. The solar-wind velocity $\mathbf{v}_{SW}$ and interplanetary magnetic field $\mathbf{B}_{IMF}$ define the direction of the convective electric field $\mathbf{E} = -\mathbf{v}_{SW} \times \mathbf{B}_{IMF}$. We indicate the $\pm E$ and $\pm B$ hemispheres as well as the coordinate axes of the Venus-Sun-Electric field reference frame described in Section 2.1. The magnetosheath is the region downstream of the bow shock containing shocked solar-wind and planetary particles.

the orientation of $\mathbf{B}_{IMF}$ with respect to the bow shock normal affects solar-wind proton flows and temperature anisotropies (Halekas et al., 2017; Rojas Mata et al., 2023). More generally, observational studies of the ~~magnetosheaths~~ magnetosheath's properties at bodies across the Solar System reveal significant dependencies on (magnetic) longitude, commonly referred to as dawn-dusk or $q_{\perp}/q_{\parallel}$ asymmetries (Dubinin et al., 2008; Dimmock and Nykyri, 2013; Walsh et al., 2014; Haaland et al., 2017; Carbary et al., 2017; Palmaerts et al., 2017; Behar et al., 2018; Rojas Mata et al., 2023). Investigating the physics behind these asymmetries has meaningfully advanced our fundamental understanding of the solar-wind interaction with the different bodies.

In contrast, few studies investigate analogous solar-wind plasma asymmetries at unmagnetized bodies as a function of latitude, i.e. between the hemispheres in which the convective electric field points away from ($+E$) or towards ($-E$) the body. At Mars, Dubinin et al. (2018) found that the magnetosheath plasma in the $+E$ hemisphere is slower and more deflected in the direction opposite to $\mathbf{E}$. Romanelli et al. (2020) determined that this asymmetry decreases with respect to the solar-wind density and increases with respect to the cross-flow component of $\mathbf{B}_{IMF}$, which is consistent with a two-fluid description of mass loading by pick-up ions. Similar analyses based on plasma data at Venus have not been found, while magnetometer-based investigations found that the magnitude of $\mathbf{B}_{IMF}$ throughout the magnetic barrier is greater in the $+E$ hemisphere (Phillips et al., 1986; Zhang et al., 1991b; Du et al., 2013; Xiao et al., 2018). Additionally, at both planets $\mathbf{B}_{IMF}$ wraps asymmetrically (e.g. more tightly in the $-E$ hemisphere) in the magnetosheath and magnetotail (Zhang et al., 2010; Du et al., 2013; Dubinin

et al., 2019, 2021; Zhang et al., 2022). Other studies which mention differences between the $\pm E$ hemispheres instead focus on the dynamics of pick-up ion escape (Barabash et al., 2007b, a; Dubinin et al., 2011; Xu et al., 2023), which at Venus has been linked to the $\mathbf{B}_{IMF}$ asymmetries (Luhmann et al., 1985; Phillips et al., 1987).

In parallel, numerical studies of the plasma environment around unmagnetized bodies have investigated topics such as hemispheric asymmetries, plasma boundary morphology, and pick-up ion dynamics (Brecht and Ferrante, 1991; Moore et al., 1991; Shimazu, 1999; Kallio et al., 2011). For example, recent hybrid models (Kallio et al., 2006; Jarvinen et al., 2013, 2016) reproduce observed $\pm E$ asymmetries concerning plasma velocities and magnetic fields, as well as indicate that the dynamics of pick-up ions depend on their upstream Larmor radius

$$r_{L,i} = \frac{m_i}{q_i} \frac{|\mathbf{v}_{SW}| B_y}{B_{IMF}^2}, \tag{1}$$

where m_i is the ion mass, q_i the ion charge, and B_y the cross-flow component of $\mathbf{B}_{IMF}$. Though the asymmetries and pick-up ions may be linked, their exact interdependence remains unresolved as asymmetries arise even if planetary ions (O^+ and H^+) are not included in the simulation (Brecht, 1990; Jarvinen et al., 2013). Additionally, few studies directly compare global simulations to local spacecraft data, so how well the models quantitatively reproduce the measured spatial structure of the plasma environment is not fully determined.

The above illustrates the opportunity to develop new insight into magnetosheath physics by comparing observations and simulations not only at a single body, but also across different bodies (i.e. Venus, Mars, and even comets). To this end, in this paper we characterize the proton plasma asymmetries between the $+E$ and $-E$ hemispheres of Venus' dayside magnetosheath. We apply and extend the methodology Rojas Mata et al. (2023) developed to statistically quantify asymmetries. In Sect. 2 we overview the data set used as well as the methodology for quantifying parameter asymmetries; our results follow in Sect. 3. We discuss connections to relevant numerical and observational studies in Sect. 4 and present concluding remarks in Sect. 5.

2 Data and methodology

2.1 Dayside magnetosheath database

For this study we use a database of proton plasma bulk-parameter measurements in Venus' dayside magnetosheath (Rojas Mata and Futaana, 2022). Based on measurements taken by the Ion Mass Analyser (IMA) instrument (Barabash et al., 2007c) and the Magnetometer (MAG) (Zhang et al., 2006) on board the Venus Express (VEX) mission (Svedhem et al., 2007), the database includes densities, velocities, and both perpendicular and parallel temperatures for 1181 locations in the magnetosheath along with ~~the upstream solar wind~~ corresponding upstream solar-wind conditions for the 597 orbits spanned. These bulk parameters result from bi-Maxwellian gyrotropic fits to IMA's velocity-distribution-function (VDF) measurements (Bader et al., 2019; Rojas Mata et al., 2022). Using fits instead of taking velocity-space moments "has the advantage of compensating for an incomplete sampling of the VDF due to IMA's limited field of view" (Rojas Mata et al., 2022), though only to a reasonable degree of blockage. Therefore, a variety of physical, statistical, and instrument-based criteria filtered out scans whose measurements were not adequately represented by a bi-Maxwellian model, either due to blockage or other reasons. As

detailed in Rojas Mata et al. (2023), the ~~database includes data only from~~ special database of Rojas Mata and Futaana (2022) was constructed by manually searching for orbits with identifiable dayside bow-shock crossings ~~and~~ in order to properly classify IMA-scan locations. Further manual selection yielded the 597 orbits which have well-defined ~~upstream solar wind conditions~~ solar-wind conditions based on medians of measurements immediately upstream of the dayside bow-shock crossing.

To characterize asymmetries between the $\pm E$ hemispheres of the magnetosheath we use the Venus-Sun-Electric field (VSE) reference frame. The $+X_{VSE}$ axis points against the solar-wind velocity, whose aberration we correct for using each orbit's upstream measurements (Rojas Mata et al., 2023). The $+Y_{VSE}$ axis points along the cross-flow component of $\mathbf{B}_{IMF}$, making $+Z_{VSE}$ point along the upstream convective electric field ~~$\mathbf{E} = -\mathbf{v}_{SW} \times \mathbf{B}_{IMF}$~~ $\mathbf{E}$. The $\pm E$ hemispheres then correspond to the north ($+Z_{VSE}$) and south ($-Z_{VSE}$) hemispheres of this reference frame. The spatial coverage of the measurements in this reference frame is decently uniform except for limited coverage on the dayside close to the subsolar point caused by VEX's orbit geometry (see the 'subsolar-wind hole' in Fig. 4 of Rojas Mata et al. (2023)).

2.2 Statistically quantifying asymmetries

Since VEX's highly-elliptical, quasi-polar orbit lead to the sampling of opposing VSE hemispheres under different solar-wind conditions, measurement-by-measurement pairing is not possible in order to quantify spatial asymmetries. Rojas Mata et al. (2023) addressed this challenge by developing a methodology which uses distributions of ratios of estimated measurement distributions as measures of the plasma parameter asymmetries. The technique also quantifies the variability of the asymmetries, provides flexibility for analyzing spatially binned data, and does not rely on models for the distributions. We refer the reader to the reference for the full discussion of the methodology; here we briefly overview the steps for quantifying the spatial asymmetry of a parameter a (e.g. speed or magnetic-field strength) between hemispheres $H1$ and $H2$:

1. Normalize the measurements of a by their corresponding value in the upstream solar wind, i.e. $\widehat{a} = a/a_{SW}$
2. Approximate the probability distribution function (PDF) of $\widehat{a}$ in each hemisphere using Gaussian kernel density estimates
3. Draw $\mathcal{O}(10^6)$ random samples each of $\widehat{a}_{H1}$ and $\widehat{a}_{H2}$ using the estimated PDFs
4. Compute the distribution of $\overline{a} = \widehat{a}_{H1}/\widehat{a}_{H2}$ by pairing the samples

In this work $H1 = +E$ hemisphere and $H2 = -E$ hemisphere of the dayside magnetosheath. The process can also be applied to binned data (e.g. between two bins centered at corresponding latitudes in each hemisphere), so we also compute asymmetries with the measurements sorted in 15°-wide latitudinal bins with a 50% overlap. Note that such binning means that we average over radial distance and longitude. The bulk statistical quantities (e.g. medians) derived from the distribution of $\overline{a}$ are superior products to those calculated by the alternative method of taking the ratio of the quantity between corresponding bins or hemispheres; such a method has higher uncertainty and worse reproducibility (Brody et al., 2002).

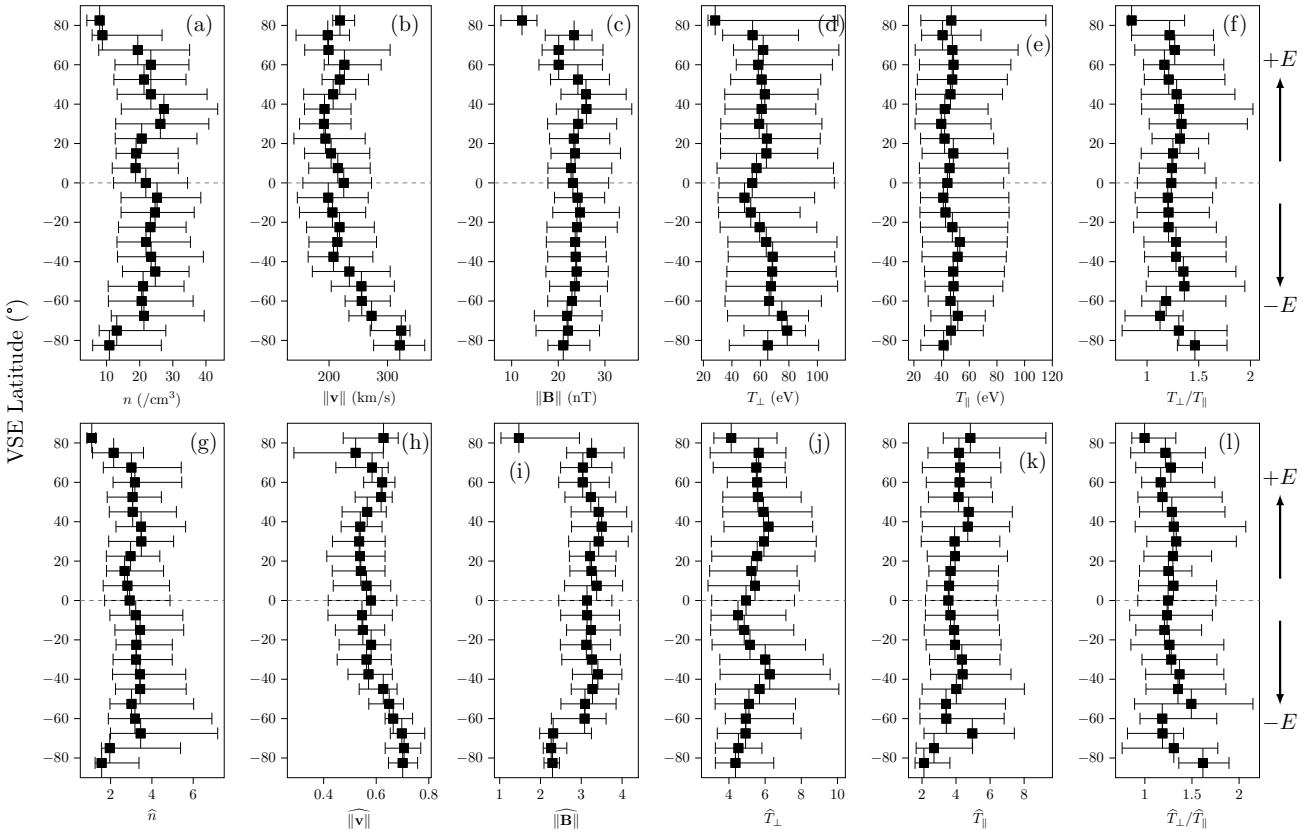

Figure 2. Proton parameters in the dayside magnetosheath as a function of latitudinal distance from the central parallel. The top row shows unnormalized values, the bottom row normalized by the solar-wind value. Positive VSE latitude corresponds to the $+E$ hemisphere, negative to the $-E$ hemisphere. Markers indicate medians while 'error' bars correspond to the first and third quartiles.

3 Results

3.1 Scalar parameters

We present in Fig. 2 the medians of the magnetosheath measurements (top row) and of their normalized values (bottom row) as of function of VSE latitude. The 'error' bars indicate the first and third quartiles of the measurement distributions in each bin; rather than uncertainty, these values reflect the spread of the distributions and how they shift across bins. Bins centered less than 60° (45°) from the central parallel contain more than 70 (100) scans each. Bins 75° or farther contain much fewer scans (< 25) so these data may have lower statistical reliability. Including them or not in the subsequent analysis, however, does not affect the final results and conclusions.

The plasma speed appears lower closer to the central parallel (Fig. 2h), which is consistent with the expectation of higher deceleration closer to the near-sub-solar-wind region (Spreiter and Alksne, 1966; Spreiter et al., 1970). Other parameters do

not seem to exhibit clear trends as a function of latitude, especially given their wide variability. We display in Fig. 3 the median parameter asymmetries as a function of latitudinal distance from the central parallel. Additionally, the top marker in each plot indicates the overall asymmetry calculated using data across all latitudes in each hemisphere. ~~Despite the larger asymmetries observed~~ Most parameters exhibit weak or insignificant asymmetries except in the bins above 60°~~(which~~, which again contain much fewer measurements ~~than the others), most parameters exhibit weak or insignificant asymmetries~~and may be less statistically reliable. The plasma speed is ~~higher~~ slightly higher ($\sim 6\%$) in the $-E$ hemisphere (Fig. 3b) while the IMF magnitude ~~is slightly higher in~~ seems more symmetric but still favors the $+E$ hemisphere ~~. Both of these asymmetries have been observed before (Phillips et al., 1986; Zhang et al., 1991b; Du et al., 2013; Dubinin et al., 2018; Xiao et al., 2018; Xu et al., 2023) . The slightly~~ by $\sim 5\%$ (Fig. 3c). This contrasts with previous observations of clear higher speeds in the $-E$ hemisphere and stronger magnetic fields in the $+E$ hemisphere (Phillips et al., 1986; Zhang et al., 1991b; Du et al., 2013; Dubinin et al., 2018; Xiao et al., . Meanwhile, the $\sim 10\%$ lower density observed at lower latitudes in the $+E$ hemisphere ~~maybe has connections to studies about~~ (Fig. 3a) may relate to plasma depletion in the magnetic barrier (Zwan and Wolf, 1976; Zhang et al., 1991a; Luhmann, 1995)~~;~~. However, even if we did not average over radial distance, the spatial resolution of the IMA scans (0.2-0.3 R_V with R_V the Venus radius) is insufficient to properly discern this effect given the expected thickness of such a plasma depletion layer (less than 1000 km). ~~The perpendicular and parallel temperatures exhibit the clearest symmetry between hemispheres (both overall and as~~ As a function of latitude~~)~~, both temperatures (Fig. 3de) appear quite symmetric; the parallel temperature has no overall asymmetry while the perpendicular temperature favors the $+E$ hemisphere by $\sim 5\%$. The temperature anisotropy (Fig. 3f) exhibits more variability but overall there ~~still does not seem to be any~~ is no significant asymmetry.

These results contrast with the asymmetries between ~~magnetosheaths~~ the magnetosheath plasma downstream of different bow-shock geometries (see Fig. 6 in Rojas Mata et al. (2023)) which are more significant and exhibit trends with upstream Alfvén Mach number. This indicates that the convective electric field has little influence on average magnetosheath properties, especially compared to the bow shock geometry. ~~Given~~ We also did not find significant trends with any upstream parameter (density, speed, Alfvén Mach number, etc.). Despite the potential connection between $\pm E$ asymmetries and pick-up ion dynamics, we ~~also checked for~~ found no significant dependencies on upstream O^+ Larmor radius~~yet none of the parameters exhibited a significant trend~~. However, since varying the upstream Larmor radius changes the direction of the pick-up ion trajectories (Jarvinen et al., 2016), analyzing the components of the bulk velocity likely yields more informative results on the matter. This requires us to ~~to~~ reevaluate our methodology to make it adequate for quantities which are not strictly positive.

3.2 Bulk-velocity components

~~We here consider~~ Fig. 4 presents the measurement distributions of v_x, v_y, and v_z in the $+E$ and $-E$ hemispheres~~presented in Fig. 4. We also display~~ , as well as the distributions for the data subsets corresponding to large (above the third quartile 1.58 R_V) and small (below the first quartile 0.75 R_V) upstream O^+ Larmor radius r_{L,O^+} (the median for all data is 1.09 R_V). We also indicate the median ~~and quartiles~~ (marker) and quartiles ('error' bars) for each distribution at the top of each plot. ~~We note~~ Note that only v_x ~~could~~ can be normalized by its upstream value since the solar wind points solely along X_{VSE}~~; we thus~~ , so we only consider unnormalized measurements. As expected, v_x is negative and larger than the other components.

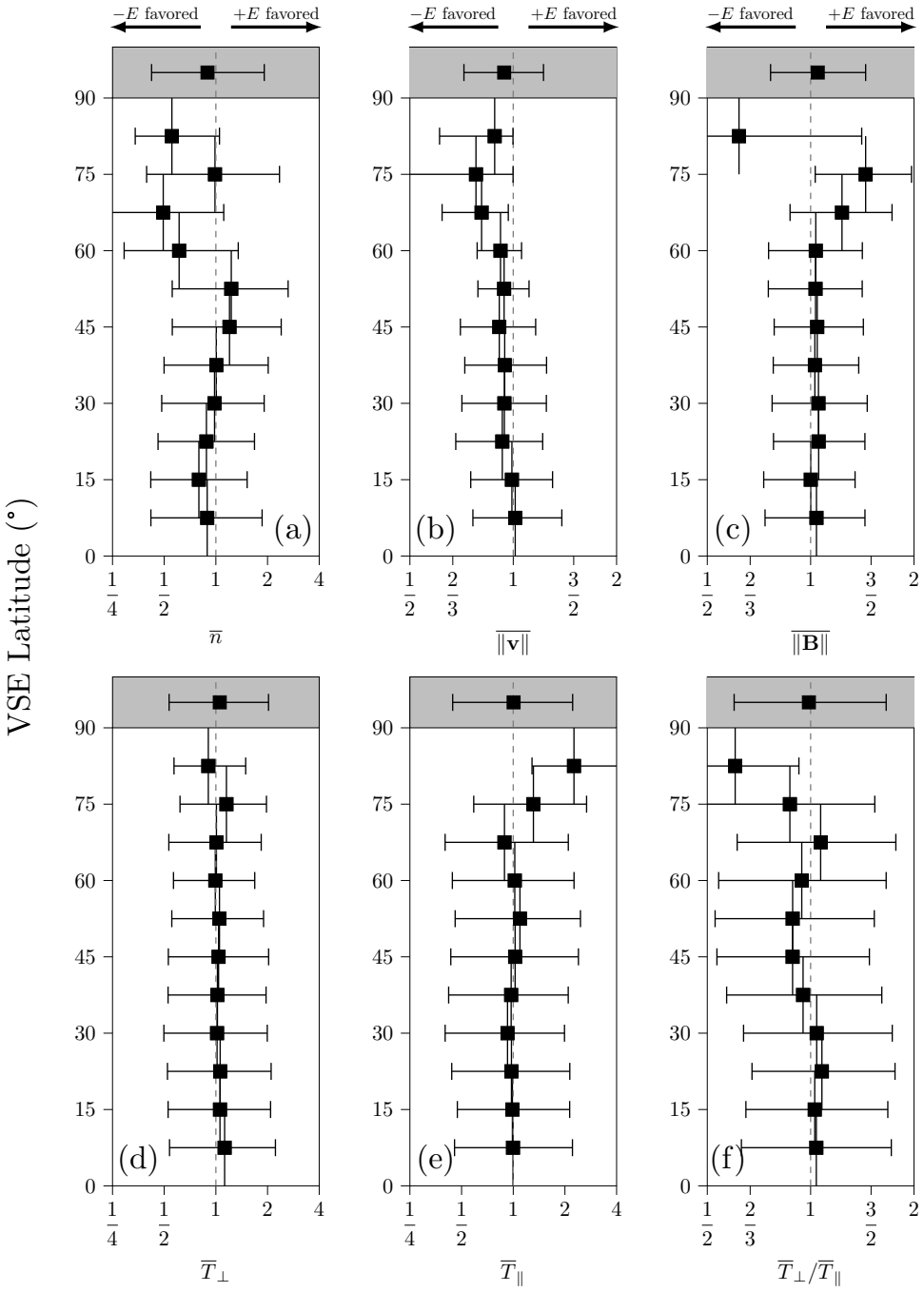

Figure 3. Proton parameter asymmetries as a function of latitudinal distance from the central parallel. The marker at the top corresponds to the overall asymmetry across all latitudes for each hemisphere. The asymmetry favors the $+E$ hemisphere if $\overline{a} > 1$ and the $-E$ hemisphere if $\overline{a} < 1$. Markers indicate medians while 'error' bars correspond to the first and third quartiles. Note the varying horizontal scales.

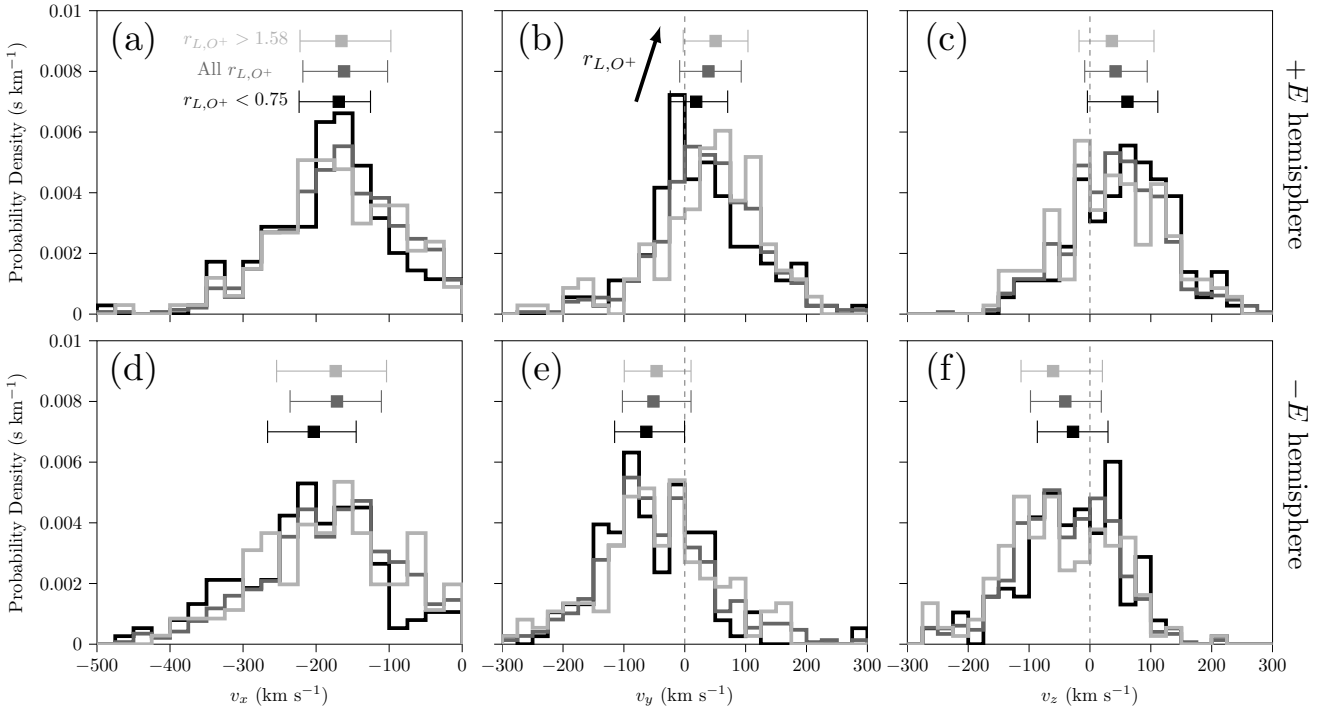

Figure 4. Distributions of the proton bulk velocity components in the $+E$ (top row) and $-E$ (bottom row) hemispheres. Black is for data with $r_{L,O^+} < 0.75R_V$, dark gray for all r_{L,O^+}, and light gray for $r_{L,O^+} > 1.58R_V$. The markers indicate the median for each distribution along with the respective first and third quartiles as the 'error' bars. The arrow indicates increasing r_{L,O^+}.

v_y is unevenly distributed about 0 due to a previously observed asymmetry in the proton flow in the VSO frame attributed to the planet's orbital motion (Lundin, 2011). Since VEX only sampled the northern VSO hemisphere, this asymmetry does not average out when converting into the VSE frame, leading to mostly positive (negative) values in the $+E$ ($-E$) hemisphere. Finally, while the sign of v_z is mostly as expected for each hemisphere, occasionally IMA's ~~limited~~ FOV combined with the spacecraft's orientation ~~sometimes leads~~ may lead to measurements with ~~poor constraints on~~ the 'wrong' sign. However, such interpretation assumes that v_z ~~. Reviewing~~ should always be positive (negative) in the $+E$ ($-E$) hemisphere. We did not find analogous studies presenting distributions of v_z (Romanelli et al. (2020) only discusses means), so we cannot compare to related work to gauge how justified this assumption is. Regardless, reviewing the measurements to correct v_z (if required at all) is beyond the scope of this work; our methodology and the equal impact of systematic errors on both hemispheres mitigate potential errors anyway.

v_x does not vary significantly with r_{L,O^+} in the $+E$ hemisphere. In the $-E$ hemisphere the small r_{L,O^+} measurements have a sudden dip around -100 km s^{-1} (possibly a random sampling artifact) which, if not present, would also make v_x insensitive to r_{L,O^+}. Both v_y and v_z follow opposite trends with r_{L,O^+} regardless of hemisphere: v_y becomes more positive as r_{L,O^+} increases and v_z more negative. The solar wind thus seems to deflect towards the $+Y_{VSE}$ and $-Z_{VSE}$ directions as

r_{L,O^+} increases. Since pick-up ions are more common in the $+E$ hemisphere (Phillips et al., 1987; Barabash et al., 2007b; Jarvinen et al., 2013), quantifying asymmetries of v_y and v_z as a function of r_{L,O^+} may clarify how these trends relate to the momentum exchange between solar-wind protons and planetary ions. Previously, ratios provided easily interpretable measures of asymmetry for positive scalar parameters such as density or temperature. However, the measurement distributions of v_y and v_z have positive and negative portions, so, while the methodology from Sect. 2.2 can still be applied, the resulting distributions of parameters ratios are more difficult to interpret. An alternative is to use a sum instead of a ratio as the measure of asymmetry; Romanelli et al. (2020) did so to study $\pm E$ asymmetries in v_z at Mars. As the average v_z was primarily positive in the $+E$ hemisphere and negative in the $-E$ one, summing the values between the hemispheres always gave the difference in the magnitude of this component. We therefore modify the procedure from Sect. 2.2 to use sums of unnormalized parameters as our measure of asymmetry, i.e. $\overline{a} = a_{H1} + a_{H2}$ instead of $\overline{a} = \widehat{a}_{H1}/\widehat{a}_{H2}$. Now $\overline{a} > 0$ indicates a $+E$-favored asymmetry and $\overline{a} < 0$ a $-E$-favored one. For our data, the 'bodies' of the v_y and v_z distributions have opposite signs in opposite hemispheres, so the 'bodies' of the sum distributions provides reliable measures of average asymmetries. However, as this is not true for the 'tails' of the distributions, the sum distributions may be artificially wide.

Adopting these modifications we present in Fig. 5 the medians of the v_y and v_z asymmetries across all latitudes in each hemisphere. Again the 'error' bars indicate the first and third quartiles of the distributions. We also show the results for the data subsets corresponding to large and small upstream O^+ Larmor radius. The v_y asymmetry decreases with increasing O^+ Larmor radius, suggesting that the underlying mechanism deflecting the solar wind in the y-direction either disappears or affects both hemispheres more evenly as r_{L,O^+} increases. Meanwhile, the v_z asymmetry favors the $+E$ hemisphere for small r_{L,O^+} and the $-E$ hemisphere for large r_{L,O^+}. This switch in which hemisphere the asymmetry favors may be connected to how much $\mathbf{E} \times \mathbf{B}$-drift and finite-Larmor-radius dynamics affect momentum transfer between planetary and solar-wind ions for different r_{L,O^+} ~~(see Sect. 4).~~ We note that these trends do not arise when splitting the data by high and low values for $|\mathbf{v}|$, $|\mathbf{B}_{IMF}|$, or B_y, the individual parameters which comprise r_{L,O^+}.

4 Discussion

Our interpretation of these Larmor-radius-dependent trends of solar-wind deflection at Venus benefits from comparisons with observations at Mars and comets; such comparative studies place the discussion into a broader context of solar-wind interactions with unmagnetized atmospheric bodies (see, for example, Luhmann et al. (1987); Fedorov et al. (2008); Holmstrom and Wang (2015); Jarvinen et al. (2016)). However, as mentioned before, few studies provide quantitative characterizations of plasma asymmetries between the $\pm E$ hemispheres, let alone investigate dependencies on Larmor radius. This is understandable as the Larmor radii of pick-up ions at these bodies are commonly larger than the obstacle radius. Thus, the particle motion is studied in the large-Larmor-radius limit in which other parameters are relevant. This contrasts with the range of r_{L,O^+} we observe at Venus (about 0.4–2.4 R_V), which means the data likely covers mixed dynamical regimes. This is illustrated by simulations in which pick-up ion species with Larmor radii similar to the planet radius experience both $\mathbf{E} \times \mathbf{B}$-drift and finite-Larmor-radius

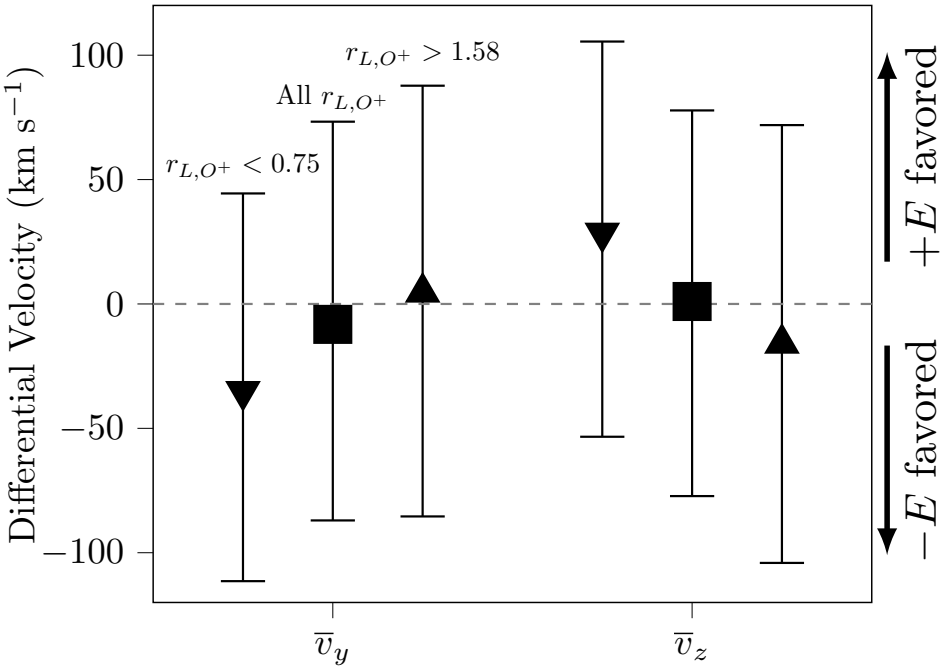

Figure 5. Proton bulk velocity component asymmetries as a function of upstream O^+ Larmor radius. For each parameter, the left marker is for $r_{L,O^+} < 0.75$, the middle for all r_{L,O^+}, and the right for $r_{L,O^+} > 1.58$. The asymmetry favors the $+E$ hemisphere if $\overline{a} > 0$ and the $-E$ hemisphere if $\overline{a} < 0$. Markers indicate the median for each distribution along with the respective first and third quartiles as the 'error' bars.

dynamics (Jarvinen et al., 2016). Fundamental differences like these complicate but do not impede drawing beneficial insight from comparisons between these bodies.

4.1 Comparison to Mars

We first compare our results to Romanelli et al. (2020)'s analysis of $\pm E$ asymmetries in the z-component of the proton bulk velocity in Mars' magnetosheath. This component was greater in magnitude in the $-E$ hemisphere, coinciding with what we observe for large r_{L,O^+} at Venus. Using a two-species ion fluid description, the authors derived an analytic expression "suggesting a dependence between the SW flow asymmetry on the $(eB_y)/(n_{SW}m_p)$ external factor", where m_p is the proton mass and n_{SW} the solar-wind density. The measured distributions of $\overline{v}_z$ indeed confirm this predicted dependence of the asymmetry on B_y, n_{SW}, and $(eB_y)/(n_{SW}m_p)$. We do not observe similar trends with respect to these parameters in the v_z asymmetry at Venus, simply verifying that the assumptions based on a large Larmor radius for planetary ions at Mars are not applicable. The authors did not investigate trends with upstream Larmor radius, thereby impeding further comparison with our analysis. Unfortunately no other studies have characterized proton plasma magnetosheath asymmetries at Mars; given the abundance of plasma data provided by missions like Mars Express (Chicarro et al., 2004; Barabash et al., 2006) or MAVEN

(Jakosky et al., 2015; Halekas et al., 2015), future work could provide new beneficial insight into the v_z asymmetry (or that of any parameter) by applying our methodology at Mars.

4.2 Comparison to simulations

As with observational work, existing numerical studies have not characterized $\pm E$ asymmetries in the magnetosheath plasma as a function of upstream Larmor radius. Nevertheless, Jarvinen et al. (2016)'s global hybrid simulations of planetary ion dynamics at Venus and Mars provide pertinent results to contextualize our observations. The authors simulated the planets' plasma environment under their respective nominal upstream conditions ("Venus nominal" and "Mars nominal"), but also with the heliodistance of each planet interchanged ("Mars at Venus" and "Venus at Mars"). By analyzing test particle trajectories of planetary ions with $m/q =$ 1, 4, 16, and 32 (i.e. H^+, He^+, O^+, and O_2^+) released at an altitude of 0.2 planet radii (see Fig. 6-9 in the reference), the authors investigated different factors affecting the $\mathbf{E} \times \mathbf{B}$-drift and finite-Larmor-radius dynamics of escaping ions. All runs feature stronger magnetic fields and O^+ ions concentrated in the $+E$ hemisphere.

The key difference in the four cases simulated is the increasing upstream O^+ Larmor radius of 0.7, 1.2, 3.0, and 5.3 planet radii (see Table 2 in the reference), the parameter chosen as a "first approximation of how important the finite-Larmor-radius effects are for the dynamics of escaping planetary ions" (Jarvinen et al., 2016). As r_{L,O^+} increases in the simulations, the O^+ trajectories in the $+E$ hemisphere align more along the $+Z_{VSE}$ axis; the pick-up ions accelerate less in the $-Y_{VSE}$ direction and more in the $+Z_{VSE}$ direction. With less pick-up ion motion along the Y_{VSE} axis, differences in the solar-wind v_y distributions between the $\pm E$ hemispheres should decrease, which is precisely the trend we see in the data in Fig. 5a. Simultaneously, the solar-wind v_z distributions in both hemispheres should become more negative, which we see in Fig. 4cf. Since v_z is mostly positive in the $+E$ hemisphere and negative in the $-E$ one, the v_z asymmetry becomes more $-E$ favored as r_{L,O^+} increases, as shown in Fig. 5a. So, despite our Venus data not spanning the same range of r_{L,O^+} as the simulations, it seems the Larmor-radius-dependent trends in the $\pm E$ asymmetries are consistent with varying momentum exchange between planetary O^+ and solar-wind protons.

Still unexplained, though, is why the v_z asymmetry is $+E$ favored for small r_{L,O^+}. We have so far only considered momentum exchange with heavy pick-up ions, yet the simulations show that the dynamics of lighter ions (like H+) are significantly different since they experience more $\mathbf{E} \times \mathbf{B}$-drift dynamics than finite-Larmor-radius effects. Light ions concentrate in the $-E$ hemisphere, so their effect would be to deflect the solar wind towards the $+Z_{VSE}$ axis. Due to their smaller mass, this may only be noticeable when the heavier ions also experience more $\mathbf{E} \times \mathbf{B}$-drift dynamics so that their contribution to momentum exchange in the Z_{VSE} direction is reduced or more even between hemispheres. New simulations expanding upon the results in Jarvinen et al. (2016) and simultaneously quantifying plasma asymmetries could provide clarity to this matter.

4.3 ~~Comparison to comet 67P/Churyumov-Gerasimenko~~

~~Behar et al. (2018)'s analysis of the solar-wind deflection at comet 67P/Churyumov-Gerasimenko provides guidance for further interpreting the v_y asymmetry. This statistical analysis of ion velocities measured during the entire Rosetta mission (Glassmeier et al., 2007; shows that the solar-wind protons are deflected towards the dusk side of the comet. The authors ascribe this effect to momentum~~

exchange with cometary ions which instead drift towards the dawn side of the comet. These results are valid for both inward and outward Parker spirals, indicating that fundamentally the cometary (solar-wind) ions are deflected towards (away from) the $\mathbf{E}\times\mathbf{B}$ direction. Since the cross-flow component of the $\mathbf{E}\times\mathbf{B}$ direction is the same for either inward or outward Parker spiral IMF, this leads to the consistent dawn/dusk deflections.

Behar et al. (2018) do not separate the data by $\pm E$ hemispheres or Larmor radius, so a direct comparison with our analysis so far is not possible. Their equations of generalized gyromotion indicate that the solar-wind deflection angle depends on the ratios of mass and density between the solar-wind and cometary ions. While we have measurements of the solar-wind proton density, we cannot readily implement reliable O^+ densities into our data set (which would serve as the analogous cometary ion densities). However, we can conduct an exploratory analysis to determine if we detect similar solar-wind deflections with respect to $\mathbf{E}\times\mathbf{B}$ direction. We must first modify the VSE frame to define a Y'_{VSE} axis which points anti-parallel to the cross-flow component of the $\mathbf{E}\times\mathbf{B}$ direction. As illustrated in Fig. **??**, inward Parker spirals in VSO (i.e. $B_x>0$) become 'ortho-Parker' in VSE, so the solar-wind proton's v_y should become more negative (as opposed to more positive as in Behar et al. (2018)). Thus, to facilitate comparisons with observations at comet 67P, we flip the sign of the y-component of velocity for measurements with $B_x>0$. This means that momentum exchange with planetary ions moving in the $\mathbf{E}\times\mathbf{B}$ direction would always make the solar wind's y'-component distribution more positive.

Orientation of the $\mathbf{E}\times\mathbf{B}$ direction and Y'_{VSE} axis in 'Parker' (left) and 'ortho-Parker' (right) spiral configurations in the VSE frame. The black arrows indicate the directions in the X_{VSE}-Y_{VSE} plane along which planetary ions drift and solar-wind ions deflect.

We present in Fig. **??** the measurement distributions of v_x, $v_{y'}$, and v_z in the $+E$ and $-E$ hemispheres as well as for all data. Since regular MHD flow interactions also deflect solar-wind protons in the magnetosheath, one strategy to determine if any additional deflection occurs due to $\mathbf{E}\times\mathbf{B}$ drift effects is to characterize the distributions with respect to a parameter related to this drift. The gyromotion equations in Behar et al. (2018) indicate that density ratios or velocity shears between protons and O^+ ions are the most appropriate parameters to investigate, however we cannot calculate these readily. Instead, we characterize the distributions as a function of the magnitude the y'-component of the $\mathbf{E}\times\mathbf{B}$ velocity

$$|\mathbf{V}_{\mathbf{E}\times\mathbf{B},y'}| = |\mathbf{V}_{\mathbf{E}\times\mathbf{B},y}| = \left|\frac{(\mathbf{E}\times\mathbf{B})_y}{|\mathbf{B}|^2}\right| = \frac{|((-\mathbf{v}_{SW}\times\mathbf{B})\times\mathbf{B})_y|}{|\mathbf{B}|^2} = \frac{|\mathbf{v}_{SW}||B_y\cos\theta_c|}{|\mathbf{B}|} = \frac{|\mathbf{v}_{SW}||\sin 2\theta_c|}{2}.$$

While not explicitly contained in the gyromotion equations, if the O^+ ions have a higher $\mathbf{V}_{\mathbf{E}\times\mathbf{B},y'}$ to which they can accelerate, then they will deflect the solar-wind protons more. We thus also separate the data into sets with high (above upper quartile), low (below lower quartile), and all values of $V_{\mathbf{E}\times\mathbf{B},y'}$. The $v_{y'}$ distributions in Fig. **??**beh indeed shift towards more positive values as $|\mathbf{V}_{\mathbf{E}\times\mathbf{B},y'}|$ increases, suggesting that the $\mathbf{E}\times\mathbf{B}$-related deflection observed at comet 67P is also measurable at Venus. The v_z distributions exhibit no dependence on $|\mathbf{V}_{\mathbf{E}\times\mathbf{B},y'}|$, which makes sense since $\mathbf{V}_{\mathbf{E}\times\mathbf{B}}$ has no z component. In contrast, v_x increases in magnitude as $|\mathbf{V}_{\mathbf{E}\times\mathbf{B},y'}|$ increases, possibly reflecting less deceleration due to momentum exchange in the x direction. However, the deceleration at the bow shock locally depends on θ_c, so bow shock geometry effects should also be considered to explain this trend. Distributions of the proton bulk velocity components in the $+E$ (top row), $-E$ (middle row), and both (bottom row) hemispheres. Black is for data with high $|V_{\mathbf{E}\times\mathbf{B},y'}|$, dark gray for all $|V_{\mathbf{E}\times\mathbf{B},y'}|$, and light gray for low

$|V_{\mathbf{E}\times\mathbf{B},y'}|$. The markers indicate the median for each distribution along with the respective first and third quartiles as the 'error' bars. The arrow indicates increasing $|V_{\mathbf{E}\times\mathbf{B},y'}|$.

We note that the v_x and $v_{y'}$ distributions appear more sensitive to $|\mathbf{V}_{\mathbf{E}\times\mathbf{B},y'}|$ in the $-E$ hemisphere. Given the higher prevalence of pick-up in the $+E$ hemisphere (Phillips et al., 1987; Barabash et al., 2007b; Jarvinen et al., 2013), we would expect a stronger coupling between these ions and the solar-wind protons in this hemisphere instead. Although Fig. **??** displays unnormalized data and the $-E$ hemisphere has higher plasma velocities, the distributions of the velocity components normalized by $|\mathbf{v}_{SW}|$ exhibit the same general features. The same is true when we characterize the distributions (normalized or not) as a function of only $|\sin 2\theta_c|$. This shows that indeed the direction of planetary ion trajectories, which determines the direction of momentum exchange, affects the deflection of the solar-wind protons in a similar manner to what is observed at comet 67P. We wish to again quantify the asymmetry between hemispheres, however, the 'body' of the distribution of $v_{y'}$ in the $-E$ hemisphere shifts from mostly negative to mostly positive. The adequacy of the sum, difference, or ratio of the distributions as a measure of the asymmetry therefore becomes questionable. In any case, these preliminary results using the proxy parameter $V_{\mathbf{E}\times\mathbf{B},y'}$ encourage further comparisons of $\mathbf{E}\times\mathbf{B}$ dynamics between Venus and comets, especially by including the O^+ bulk properties. Comparing to the simulations by Jarvinen et al. (2016) would also add to the discussion. Unfortunately, due to the Parker spiral angles and constant solar-wind speed used, the four cases all have nearly identical values of $|\mathbf{V}_{\mathbf{E}\times\mathbf{B},y'}|$, so we cannot incorporate them into this analysis.

5 Conclusions

Using measurements taken by Venus Express' ion mass-energy spectrometer and magnetometer, in this paper we characterized proton bulk-parameter asymmetries between the $\pm E$ hemispheres of Venus' dayside magnetosheath. The main results are as follows:

1. Both density and speed are slightly higher in Speed has a weak asymmetry favoring the $-E$ hemisphere ($\sim 6\%$), whereas the magnetic-field strength is slightly higher in slightly favors the $+E$ hemisphere . by $\sim 5\%$. Previous studies have found stronger asymmetries for these two parameters.

2. No significant asymmetries exist in the temperatures or their ratio. parallel temperature or the temperature anisotropy. The density asymmetry favors the $-E$ hemisphere by $\sim 10\%$ while the perpendicular temperature favors the $+E$ hemisphere by $\sim 5\%$.

3. The y and z components of the bulk velocity and their asymmetries exhibit trends with the upstream O^+ Larmor radius. Comparison to simulations and studies at Mars suggest these trends are Mars studies suggests that these trends may be consistent with deflection by momentum exchange with planetary ions.

4. The solar-wind deflection in the y direction also exhibits trends with a proxy parameter related to the $\mathbf{E}\times\mathbf{B}$ drift of planetary ions. This again seems to result from due to momentum exchange with planetary ionsand mimics solar-wind deflection dynamics observed at comet 67P. .

Our comparative analysis ~~between Venus, Mars, and comet 67P~~ certainly has limitations yet nevertheless demonstrates the appeal of directly characterizing space plasmas across bodies of different scales. ~~New studies jointly analyzing~~ In addition to Venus and Mars, comets could be included in the analysis, for example by considering the solar-wind deflection at comet 67P/Churyumov-Gerasimenko (Behar et al., 2018). New numerical and observational analyses of the plasma environment ~~of the~~ at all these bodies through ~~simulation or observation with~~ a uniform methodology would provide further insight into the phenomena discussed here. For example, identifying the parameters controlling the various asymmetries and characterizing their effect under equivalent upstream conditions can provide a more fundamental perspective of the solar-wind interaction with unmagnetized obstacles.

Data availability. All VEX data are publicly accessible at the ESA Planetary Science Archive at https://www.cosmos.esa.int/web/psa/venus-express. The dayside magnetosheath data are available in the in-text data citation Rojas Mata and Futaana (2022).

Author contributions. SRM analyzed the data, prepared the figures, and wrote the text. GSW and YF helped with text revision. TLZ is PI of VEX MAG.

Competing interests. The authors declare that they have no conflict of interest.

Acknowledgements. SRM was funded by the Swedish National Space Agency under contracts 145/19 and 79/19.

References

Bader, A., Stenberg Wieser, G., André, M., Wieser, M., Futaana, Y., Persson, M., Nilsson, H., and Zhang, T.: Proton Temperature Anisotropies in the Plasma Environment of Venus, Journal of Geophysical Research: Space Physics, 124, 3312–3330, https://doi.org/10.1029/2019JA026619, 2019.

Barabash, S., Lundin, R., Andersson, H., Brinkfeldt, K., Grigoriev, A., Gunell, H., Holmström, M., Yamauchi, M., Asamura, K., Bochsler, P., Wurz, P., Cerulli-Irelli, R., Mura, A., Milillo, A., Maggi, M., Orsini, S., Coates, A. J., Linder, D. R., Kataria, D. O., Curtis, C. C., Hsieh, K. C., Sandel, B. R., Frahm, R. A., Sharber, J. R., Winningham, J. D., Grande, M., Kallio, E., Koskinen, H., Riihelä, P., Schmidt, W., Säles, T., Kozyra, J. U., Krupp, N., Woch, J., Livi, S., Luhmann, J. G., McKenna-Lawlor, S., Roelof, E. C., Williams, D. J., Sauvaud, J. A., Fedorov, A., and Thocaven, J. J.: The analyzer of space plasmas and energetic atoms (ASPERA-3) for the mars express mission, Space Science Reviews, 126, 113–164, https://doi.org/10.1007/s11214-006-9124-8, 2006.

Barabash, S., Fedorov, A., Lundin, R., and Sauvaud, J. A.: Martian atmospheric erosion rates, Science, 315, 501–503, https://doi.org/10.1126/science.1134358, 2007a.

Barabash, S., Fedorov, A., Sauvaud, J. J., Lundin, R., Russell, C. T., Futaana, Y., Zhang, T., Andersson, H., Brinkfeldt, K., Grigoriev, A., Holmström, M., Yamauchi, M., Asamura, K., Baumjohann, W., Lammer, H., Coates, A. J., Kataria, D. O., Linder, D. R., Curtis, C. C., Hsieh, K. C., Sandel, B. R., Grande, M., Gunell, H., Koskinen, H. E., Kallio, E., Riihelä, P., Säles, T., Schmidt, W., Kozyra, J., Krupp, N., Fränz, M., Woch, J., Luhmann, J. G., McKenna-Lawlor, S., Mazelle, C., Thocaven, J. J., Orsini, S., Cerulli-Irelli, R., Mura, M., Milillo, M., Maggi, M., Roelof, E., Brandt, P., Szego, K., Winningham, J. D., Frahm, R. A., Scherrer, J., Sharber, J. R., Wurz, P., and Bochsler, P.: The loss of ions from Venus through the plasma wake, Nature, 450, 650–653, https://doi.org/10.1038/nature06434, 2007b.

Barabash, S., Sauvaud, J. A., Gunell, H., Andersson, H., Grigoriev, A., Brinkfeldt, K., Holmström, M., Lundin, R., Yamauchi, M., Asamura, K., Baumjohann, W., Zhang, T., Coates, A. J., Linder, D. R., Kataria, D. O., Curtis, C. C., Hsieh, K. C., Sandel, B. R., Fedorov, A., Mazelle, C., Thocaven, J. J., Grande, M., Koskinen, H. E., Kallio, E., Säles, T., Riihela, P., Kozyra, J. U., Krupp, N., Woch, J., Luhmann, J. G., McKenna-Lawlor, S., Orsini, S., Cerulli-Irelli, R., Mura, M., Milillo, M., Maggi, M., Roelof, E. C., Brandt, P. C., Russell, C. T., Szego, K., Winningham, J. D., Frahm, R. A., Scherrer, J., Sharber, J. R., Wurz, P., and Bochsler, P.: The Analyser of Space Plasmas and Energetic Atoms (ASPERA-4) for the Venus Express mission, Planetary and Space Science, 55, 1772–1792, https://doi.org/10.1016/j.pss.2007.01.014, 2007c.

Behar, E., Tabone, B., and Nilsson, H.: Dawn-dusk asymmetry induced by the Parker spiral angle in the plasma dynamics around comet 67P/Churyumov-Gerasimenko, Monthly Notices of the Royal Astronomical Society, 478, 1570–1575, https://doi.org/10.1088/0035-8711/00/0/11111, 2018.

Brain, D. A., Bagenal, F., Ma, Y. J., Nilsson, H., and Stenberg Wieser, G.: Atmospheric escape from unmagnetized bodies, Journal of Geophysical Research: Planets, 121, 2364–2385, https://doi.org/10.1002/2016JE005162, 2016.

Brecht, S. H.: Magnetic asymmetries of unmagnetized planets, Geophysical Research Letters, 17, 1243–1246, https://doi.org/10.1029/GL017i009p01243, 1990.

Brecht, S. H. and Ferrante, J. R.: Global hybrid simulations of unmagnetized planets: Comparison of Venus and Mars, Journal of Geophysical Research: Space Physics, 96, 11 209–11 220, https://doi.org/10.1029/91JA00671, 1991.

Brody, J. P., Williams, B. A., Wold, B. J., and Quake, S. R.: Significance and statistical errors in the analysis of DNA microarray data, Proceedings of the National Academy of Sciences of the United States of America, 99, 12 975–12 978, https://doi.org/10.1073/pnas.162468199, 2002.

Carbary, J. F., Mitchell, D. G., Rymer, A. M., Krupp, N., Hamilton, D., Krimigis, S. M., and Badman, S. V.: Local Time Asymmetries in Saturn's Magnetosphere, chap. 25, pp. 323–336, American Geophysical Union (AGU), https://doi.org/https://doi.org/10.1002/9781119216346.ch25, 2017.

Chai, L., Wan, W., Fraenz, M., Zhang, T., Dubinin, E., Wei, Y., Li, Y., Rong, Z., Zhong, J., Han, X., and Futaana, Y.: Solar zenith angle-dependent asymmetries in Venusian bow shock location revealed by Venus Express, Journal of Geophysical Research: Space Physics, 120, 4446–4451, https://doi.org/10.1002/2015JA021221, 2015.

Chicarro, A., Martin, P., and Trautner, R.: The Mars Express Mission: An Overview, in: Mars Express: the scientific payload, edited by Wilson, A., vol. 1240, pp. 3–13, ESA Publications Division, Noordwijk, Netherlands, 2004.

Delva, M., Mazelle, C., and Bertucci, C.: Upstream ion cyclotron waves at venus and mars, Space Science Reviews, 162, 5–24, https://doi.org/10.1007/s11214-011-9828-2, 2011.

Dimmock, A. P. and Nykyri, K.: The statistical mapping of magnetosheath plasma properties based on THEMIS measurements in the magnetosheath interplanetary medium reference frame, Journal of Geophysical Research: Space Physics, 118, 4963–4976, https://doi.org/10.1002/jgra.50465, 2013.

Du, J., Zhang, T., Baumjohann, W., Wang, C., Volwerk, M., Vörös, Z., and Guicking, L.: Statistical study of low-frequency magnetic field fluctuations near Venus under the different interplanetary magnetic field orientations, Journal of Geophysical Research, 115, https://doi.org/10.1029/2010JA015549, 2010.

Du, J., Wang, C., Zhang, T., and Kallio, E.: Asymmetries of the magnetic field line draping shape around Venus, Journal of Geophysical Research: Space Physics, 118, 6915–6920, https://doi.org/10.1002/2013JA019127, 2013.

Dubinin, E., Chanteur, G., Fraenz, M., Modolo, R., Woch, J., Roussos, E., Barabash, S., Lundin, R., and Winningham, J. D.: Asymmetry of plasma fluxes at Mars. ASPERA-3 observations and hybrid simulations, Planetary and Space Science, 56, 832–835, https://doi.org/10.1016/j.pss.2007.12.006, 2008.

Dubinin, E., Fränz, M., Fedorov, A., Lundin, R., Edberg, N. J., Duru, F., and Vaisberg, O.: Ion energization and escape on mars and venus, vol. 162, https://doi.org/10.1007/s11214-011-9831-7, 2011.

Dubinin, E., Fraenz, M., Pätzold, M., Halekas, J. S., Mcfadden, J., Connerney, J. E., Jakosky, B. M., Vaisberg, O., and Zelenyi, L.: Solar Wind Deflection by Mass Loading in the Martian Magnetosheath Based on MAVEN Observations, Geophysical Research Letters, 45, 2574–2579, https://doi.org/10.1002/2017GL076813, 2018.

Dubinin, E., Modolo, R., Fraenz, M., Päetzold, M., Woch, J., Chai, L., Wei, Y., Connerney, J. E., Mcfadden, J., DiBraccio, G., Espley, J., Grigorenko, E., and Zelenyi, L.: The Induced Magnetosphere of Mars: Asymmetrical Topology of the Magnetic Field Lines, Geophysical Research Letters, 46, 12 722–12 730, https://doi.org/10.1029/2019GL084387, 2019.

Dubinin, E., Fraenz, M., Modolo, R., Pätzold, M., Tellmann, S., Vaisberg, O., Shuvalov, S., Zelenyi, L., Chai, L., Wei, Y., McFadden, J., DiBraccio, G., and Espley, J.: Induced Magnetic Fields and Plasma Motions in the Inner Part of the Martian Magnetosphere, Journal of Geophysical Research: Space Physics, 126, https://doi.org/10.1029/2021JA029542, 2021.

Edberg, N. J. T., Auster, U., Barabash, S., Bößwetter, A., Brain, D. A., Burch, J. L., Carr, C. M., H. Cowley, S. W., Cupido, E., Duru, F., Eriksson, A. I., Fränz, M., Glassmeier, K. H., Goldstein, R., Lester, M., Lundin, R., Modolo, R., Nilsson, H., Richter, I., Samara, M., and Trotignon, J. G.: Rosetta and Mars Express observations of the influence of high solar wind pressure on the Martian plasma environment, Annales Geophysicae, 27, 4533–4545, https://doi.org/10.5194/angeo-27-4533-2009, 2009.

Fedorov, A., Ferrier, C., Sauvaud, J. A., Barabash, S., Zhang, T., Mazelle, C., Lundin, R., Gunell, H., Andersson, H., Brinkfeldt, K., Futaana, Y., Grigoriev, A., Holmström, M., Yamauchi, M., Asamura, K., Baumjohann, W., Lammer, H., Coates, A. J., Kataria, D. O., Linder, D. R.,

Curtis, C. C., Hsieh, K. C., Sandel, B. R., Thocaven, J. J., Grande, M., Koskinen, H., Kallio, E., Sales, T., Schmidt, W., Riihela, P., Kozyra, J., Krupp, N., Woch, J., Luhmann, J. G., McKenna-Lawlor, S., Orsini, S., Cerulli-Irelli, R., Mura, A., Milillo, A., Maggi, M., Roelof, E., Brandt, P., Russell, C. T., Szego, K., Winningham, J. D., Frahm, R. A., Scherrer, J., Sharber, J. R., Wurz, P., and Bochsler, P.: Comparative analysis of Venus and Mars magnetotails, Planetary and Space Science, 56, 812–817, https://doi.org/10.1016/j.pss.2007.12.012, 2008.

Futaana, Y., Stenberg Wieser, G., Barabash, S., and Luhmann, J. G.: Solar Wind Interaction and Impact on the Venus Atmosphere, Space Science Reviews, 212, 1453–1509, https://doi.org/10.1007/s11214-017-0362-8, 2017.

Glassmeier, K. H., Boehnhardt, H., Koschny, D., Kührt, E., and Richter, I.: The Rosetta mission: Flying towards the origin of the solar system, Space Science Reviews, 128, 1–21, https://doi.org/10.1007/s11214-006-9140-8, 2007.

Haaland, S., Runov, A., and Forsyth, C., eds.: Dawn-Dusk Asymmetries in Planetary Plasma Environments, American Geophysical Union (AGU), https://doi.org/10.1002/9781119216346, 2017.

Halekas, J. S., Taylor, E. R., Dalton, G., Johnson, G., Curtis, D. W., McFadden, J. P., Mitchell, D. L., Lin, R. P., and Jakosky, B. M.: The Solar Wind Ion Analyzer for MAVEN, Space Science Reviews, 195, 125–151, https://doi.org/10.1007/s11214-013-0029-z, 2015.

Halekas, J. S., Brain, D. A., Luhmann, J. G., DiBraccio, G. A., Ruhunusiri, S., Harada, Y., Fowler, C. M., Mitchell, D. L., Connerney, J. E., Espley, J. R., Mazelle, C., and Jakosky, B. M.: Flows, Fields, and Forces in the Mars-Solar Wind Interaction, Journal of Geophysical Research: Space Physics, 122, 11,320–11,341, https://doi.org/10.1002/2017JA024772, 2017.

Holmstrom, M. and Wang, X. D.: Mars as a comet: Solar wind interaction on a large scale, Planetary and Space Science, 119, 43–47, https://doi.org/10.1016/j.pss.2015.09.017, 2015.

Jakosky, B. M., Lin, R. P., Grebowsky, J. M., Luhmann, J. G., Mitchell, D. F., Beutelschies, G., Priser, T., Acuna, M., Andersson, L., Baird, D., Baker, D., Bartlett, R., Benna, M., Bougher, S., Brain, D., Carson, D., Cauffman, S., Chamberlin, P., Chaufray, J. Y., Cheatom, O., Clarke, J., Connerney, J., Cravens, T., Curtis, D., Delory, G., Demcak, S., Dewolfe, A., Eparvier, F., Ergun, R., Eriksson, A., Espley, J., Fang, X., Folta, D., Fox, J., Gomez-Rosa, C., Habenicht, S., Halekas, J., Holsclaw, G., Houghton, M., Howard, R., Jarosz, M., Jedrich, N., Johnson, M., Kasprzak, W., Kelley, M., King, T., Lankton, M., Larson, D., Leblanc, F., Lefevre, F., Lillis, R., Mahaffy, P., Mazelle, C., McClintock, W., McFadden, J., Mitchell, D. L., Montmessin, F., Morrissey, J., Peterson, W., Possel, W., Sauvaud, J. A., Schneider, N., Sidney, W., Sparacino, S., Stewart, A. I., Tolson, R., Toublanc, D., Waters, C., Woods, T., Yelle, R., and Zurek, R.: The Mars Atmosphere and Volatile Evolution (MAVEN) Mission, Space Science Reviews, 195, 3–48, https://doi.org/10.1007/s11214-015-0139-x, 2015.

Jarvinen, R., Kallio, E., and Dyadechkin, S.: Hemispheric asymmetries of the Venus plasma environment, Journal of Geophysical Research: Space Physics, 118, 4551–4563, https://doi.org/10.1002/jgra.50387, 2013.

Jarvinen, R., Brain, D. A., and Luhmann, J. G.: Dynamics of planetary ions in the induced magnetospheres of Venus and Mars, Planetary and Space Science, 127, 1–14, https://doi.org/10.1016/j.pss.2015.08.012, 2016.

Kallio, E., Jarvinen, R., and Janhunen, P.: Venus-solar wind interaction: Asymmetries and the escape of O+ ions, Planetary and Space Science, 54, 1472–1481, https://doi.org/10.1016/j.pss.2006.04.030, 2006.

Kallio, E., Chaufray, J. Y., Modolo, R., Snowden, D., and Winglee, R.: Modeling of venus, mars, and titan, Space Science Reviews, 162, 267–307, https://doi.org/10.1007/s11214-011-9814-8, 2011.

Longmore, M., Schwartz, S. J., Geach, J., Cooling, B. M., Dandouras, I., Lucek, E. A., and Fazakerley, A. N.: Dawn-dusk asymmetries and sub-Alfvénic flow in the high and low latitude magnetosheath, Annales Geophysicae, 23, 3351–3364, https://doi.org/10.5194/angeo-23-3351-2005, 2005.

Lucek, E. A., Constantinescu, D., Goldstein, M. L., Pickett, J., Pinçon, J. L., Sahraoui, F., Treumann, R. A., and Walker, S. N.: The magnetosheath, Space Science Reviews, 118, 95–152, https://doi.org/10.1007/s11214-005-3825-2, 2005.

Luhmann, J. G.: The inner magnetosheath of Venus: An analogue for Earth?, Journal of Geophysical Research, 100, 12,035–13,045, 1995.

Luhmann, J. G., Russell, C. T., Spreiter, J. R., and Stahara, S. S.: Evidence for mass-loading of the Venus magnetosheath, Advances in Space Research, 5, 307–311, https://doi.org/10.1016/0273-1177(85)90155-3, 1985.

Luhmann, J. G., Russell, C. T., Phillips, J. L., and Barnes, A.: On the role of the quasi-parallel bow shock in ion pickup: A lesson from Venus?, Journal of Geophysical Research, 92, 2544–2550, https://doi.org/10.1029/ja092ia03p02544, 1987.

Lundin, R.: Ion acceleration and outflow from mars and venus: An overview, Space Science Reviews, 162, 309–334, https://doi.org/10.1007/s11214-011-9811-y, 2011.

Moore, K. R., Thomas, V. A., and McComas, D. J.: Global hybrid simulation of the solar wind interaction with the dayside of Venus, Journal of Geophysical Research: Space Physics, 96, 7779–7791, https://doi.org/10.1029/91JA00013, 1991.

Nilsson, H., Lundin, R., Lundin, K., Barabash, S., Borg, H., Norberg, O., Fedorov, A., Sauvaud, J. A., Koskinen, H., Kallio, E., Riihelä, P., and Burch, J. L.: RPC-ICA: The ion composition analyzer of the Rosetta plasma consortium, Space Science Reviews, 128, 671–695, https://doi.org/10.1007/s11214-006-9031-z, 2007.

Palmaerts, B., Vogt, M. F., Krupp, N., Grodent, D., and Bonfond, B.: Dawn-Dusk Asymmetries in Jupiter's Magnetosphere, chap. 24, pp. 307–322, American Geophysical Union (AGU), https://doi.org/https://doi.org/10.1002/9781119216346.ch24, 2017.

Phillips, J. L., Luhmann, J. G., Russell, C. T., and Alexander, C. J.: Interplanetary magnetic field control of the Venus magnetosheathfield and bow shock location, Advances in Space Research, 6, 179–183, https://doi.org/10.1016/0273-1177(86)90030-X, 1986.

Phillips, J. L., Luhmann, J. G., Russell, C. T., and Moore, K. R.: Finite Larmor radius effect on ion pickup at Venus, Journal of Geophysical Research, 92, 9920, https://doi.org/10.1029/ja092ia09p09920, 1987.

Rojas Mata, S. and Futaana, Y.: Proton Plasma Bulk-Parameter Measurements in Venus' Dayside Magnetosheath, https://doi.org/10.5878/4wfd-pj36, 2022.

Rojas Mata, S., Stenberg Wieser, G., Futaana, Y., Bader, A., Persson, M., Fedorov, A., and Zhang, T.: Proton Temperature Anisotropies in the Venus Plasma Environment During Solar Minimum and Maximum, Journal of Geophysical Research: Space Physics, 127, https://doi.org/10.1029/2021JA029611, 2022.

Rojas Mata, S., Stenberg Wieser, G., Futaana, Y., and Zhang, T.: Proton Plasma Asymmetries Between Venus ' Quasi-Perpendicular and Quasi-Parallel Magnetosheaths Journal of Geophysical Research : Space Physics, Journal of Geophysical Research: Space Physics, 128, 1–16, https://doi.org/10.1029/2022JA031149, 2023.

Romanelli, N., DiBraccio, G., Halekas, J., Dubinin, E., Gruesbeck, J., Espley, J., Poh, G., Ma, Y., and Luhmann, J. G.: Variability of the Solar Wind Flow Asymmetry in the Martian Magnetosheath Observed by MAVEN, Geophysical Research Letters, 47, https://doi.org/10.1029/2020GL090793, 2020.

Ruhunusiri, S., Halekas, J. S., Espley, J. R., Mazelle, C., Brain, D., Harada, Y., DiBraccio, G. A., Livi, R., Larson, D. E., Mitchell, D. L., Jakosky, B. M., and Howes, G. G.: Characterization of turbulence in the Mars plasma environment with MAVEN observations, Journal of Geophysical Research: Space Physics, 122, 656–674, https://doi.org/10.1002/2016JA023456, 2017.

Russell, C. T., Luhmann, J. G., and Strangeway, R. J.: Space Physics: An Introduction, Cambridge University Press, 2016.

Shimazu, H.: Three-dimensional hybrid simulation of magnetized plasma flow around an obstacle, Earth, Planets and Space, 51, 383–393, https://doi.org/10.1186/BF03352242, 1999.

Signoles, C., Persson, M., Futaana, Y., Aizawa, S., André, N., Bergman, S., Fedorov, A., Mazelle, C., Rojas Mata, S., Wolff, A., and Zhang, T.: Influence of Solar Wind Variations on the Shapes of Venus ' Plasma Boundaries Based on Venus Express Observations, The Astrophysical Journal, 95, https://doi.org/10.3847/1538-4357/ace7b1, 2023.

Spreiter, J. R. and Alksne, A. Y.: Hydrodynamic flow around the magnetosphere, Planetary and Space Science, 14, 223–253, https://doi.org/10.1016/0032-0633(66)90124-3, 1966.

Spreiter, J. R., Summers, A. L., and Rizzi, A. W.: Solar Wind Flow past Nonmagnetic Planets – Venus and Mars, Planetary and Space Science, 18, 1281–1299, 1970.

Svedhem, H., Titov, D. V., McCoy, D., Lebreton, J. P., Barabash, S., Bertaux, J. L., Drossart, P., Formisano, V., Häusler, B., Korablev, O., Markiewicz, W. J., Nevejans, D., Pätzold, M., Piccioni, G., Zhang, T., Taylor, F. W., Lellouch, E., Koschny, D., Witasse, O., Eggel, H., Warhaut, M., Accomazzo, A., Rodriguez-Canabal, J., Fabrega, J., Schirmann, T., Clochet, A., and Coradini, M.: Venus Express - The first European mission to Venus, Planetary and Space Science, 55, 1636–1652, https://doi.org/10.1016/j.pss.2007.01.013, 2007.

Walsh, A. P., Haaland, S., Forsyth, C., Keesee, A. M., Kissinger, J., Li, K., Runov, A., Soucek, J., Walsh, B. M., Wing, S., and Taylor, M. G.: Dawn-dusk asymmetries in the coupled solar wind-magnetosphere-ionosphere system: A review, Annales Geophysicae, 32, 705–737, https://doi.org/10.5194/angeo-32-705-2014, 2014.

Xiao, S. D., Zhang, T., and Vörös, Z.: Magnetic Fluctuations and Turbulence in the Venusian Magnetosheath Downstream of Different Types of Bow Shock, Journal of Geophysical Research: Space Physics, 123, 8219–8226, https://doi.org/10.1029/2018JA025250, 2018.

Xu, Q., Xu, X., Zuo, P., Futaana, Y., Chang, Q., and Gu, H.: Solar Control of the Pickup Ion Plume in the Dayside Magnetosheath of Venus, Geophysical Research Letters, 50, 1–9, https://doi.org/10.1029/2022GL102401, 2023.

Zhang, C., Rong, Z., Klinger, L., Nilsson, H., Shi, Z., He, F., Gao, J., Li, X., Futaana, Y., Ramstad, R., Wang, X., Holmström, M., Barabash, S., Fan, K., and Wei, Y.: Three-Dimensional Configuration of Induced Magnetic Fields Around Mars, Journal of Geophysical Research Planets, 127, https://doi.org/10.1029/2022JE007334, 2022.

Zhang, T., Luhmann, J. G., and Russell, C. T.: The Magnetic Barrier at Venus, Journal of Geophysical Research: Space Physics, 96, 11 145–11 153, 1991a.

Zhang, T., Schwingenschuh, K., Russell, C. T., and Luhmann, J. G.: Asymmetries in the Location of the Venus and Mars Bow Shock, Geophysical Research Letters, 18, 127–129, 1991b.

Zhang, T., Baumjohann, W., Delva, M., Auster, H.-U., Balogh, A., Russell, C. T., Barabash, S., Balikhin, M. A., Berghofer, G., Biernat, H. K., Lammer, H., Lichtenegger, H., Magnes, W., Nakamura, R., Penz, T., Schwingenschuh, K., Vörös, Z., Zambelli, W., Fornacon, K.-H., Glassmeier, K.-H., Richter, I., Carr, C., Kudela, K., Shi, J. K., Zhao, H., Motschmann, U., and Lebreton, J.-P.: Magnetic field investigation of the Venus plasma environment: Expected new results from Venus Express, Planetary and Space Science, 54, 1336–1343, https://doi.org/https://doi.org/10.1016/j.pss.2006.04.018, 2006.

Zhang, T., Baumjohann, W., Du, J., Nakamura, R., Jarvinen, R., Kallio, E., Du, A. M., Balikhin, M. A., Luhmann, J. G., and Russell, C. T.: Hemispheric asymmetry of the magnetic field wrapping pattern in the Venusian magnetotail, Geophysical Research Letters, 37, https://doi.org/10.1029/2010GL044020, 2010.

Zwan, B. J. and Wolf, R. A.: Depletion of Solar Wind Plasma Near a Planetary Boundary, Journal of Geophysical Research, 81, 1636–1648, https://doi.org/10.1029/ja081i010p01636, 1976.